Hindawi Publishing Corporation
Journal of Chemistry
Volume 2016, Article ID 6918294, 8 pages
http://dx.doi.org/10.1155/2016/6918294

Research Article

On the Electronic Effect of V, Fe, and Ni on MgO(100) and BaO(100) Surface: An Explanation from a Periodic Density Functional

Rafael Añez and Aníbal Sierraalta

Laboratorio de Química Física y Catálisis Computacional, Centro de Química, Instituto Venezolano de Investigaciones Científicas, Caracas 21827, Venezuela

Correspondence should be addressed to Rafael Añez; ranez@ivic.gob.ve

Received 6 December 2015; Revised 7 January 2016; Accepted 17 January 2016

Academic Editor: Zhongfang Chen

A periodic density functional study of the V, Fe, and Ni sublayer doped MgO(100) and BaO(100) surfaces was carried out using a periodic approach in the context of the GGA approximation. Results suggest that doping atoms accommodate better in the MgO than in BaO because covalent radii of the doping atoms are closer to that of the Mg atom. Sizes of the doping atom, bulk forces, and electronic effects play an important role in the structural changes observed in doped surfaces studied herein. From all the doped studies, Ni doped Ba(100) surface is shown to be a promising material for trapping molecules with partially occupied states.

1. Introduction

Alkaline earth metal oxides (AEMO) have been studied in the last years for their ability to trap atmospheric gases as NO_X and CO_X [1, 2]. The capability of adsorbing molecules is due to its high Lewis basicity which increases as the alkaline earth metal becomes larger and more electropositive [3]. Superbase sites can be generated promoting the surface with zero-valent alkali metals [4]. Zero-valent alkali metals donate one electron to the lattice which is localized in the defective site and displays similar electron density characteristics such as an oxygen vacancy (F^+ center) [5]. The basicity of these sites is such that NO is transformed to paramagnetic NO_2^{2-}; these molecules are easily detected by the ESR technique [6].

Apart from the alkali metals, other elements can dope the crystalline structure of the AEMO. Raschman and Fedoročková [7], using atomic absorption spectroscopy, found that low concentration of CaO, Fe_2O_3, Al_2O_3, and SiO_2 are present in natural MgO. These elements, as in the case of alkali metals, affect the basicity of the AEMO and hence the activity of these materials when they are used as catalysts or trapping materials. Ueda et al. [8, 9] studied the reaction of nitriles with methanol to form α, β-unsaturated nitriles using different M-MgO catalysts (M = Al, Fe, Cr, Mn, Ni, and Cu). The authors found that whereas MgO was practically unable to transform acetonitrile, doped MgO displayed some activity and, depending on the doping, the selectivity can change to acrylonitrile or propionitrile. A more recent study of the NO_X storage and reduction over Pt-BaO/Al_2O_3 catalysts showed that it is possible to modify the storage-reduction selectivity controlling the Pt concentration [10]. Then, the alkali or transition metal atoms transform the electronic environment of the AEMO surfaces producing changes in their basicity which modify their performance for the molecular adsorption.

From a theoretical point of view, only few works are found in the literature about metal doped AEMO. Halim et al. [11], using embedded clusters in the context of density functional theory (DFT), found that defective sites and surface doped with transition metal atoms drastically enhance the adsorption of CO on AEMO. Baltrusaitis et al. [12], by the use of a periodic DFT approach, studied the adsorption of NO_2, CO_2, and SO_2 on Ca and Fe doped MgO(100) surface. Because self-diffusion [13] or counterdiffusion [14] could occurs in AEMO, the doped surfaces were built replacing a Mg atom of the second layer of an undefected surface by an Ca or

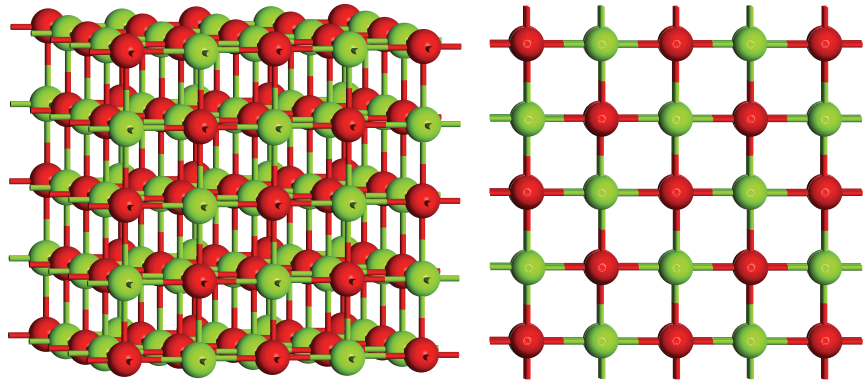

(a) (b)

Figure 1: Lateral (a) and top (b) views of the slab used for all calculations. Oxygen atoms in red balls and metal atoms in green balls.

Fe atom. The authors found that, despite the depth of the doped, the surfaces displayed an enhanced adsorption in comparison with the undoped surfaces. These results showed as the doping affects the electronic environment of the surface even when the metal atom diffuses to more internal layers. In a previous work, we studied the interaction of NO on defective Au doped BaO(100) surface [15] using a periodic DFT approach. We found that overlap of the density of states (DOS) between the surface and the adsorbate gives a qualitative point of view of the adsorption energy; then adsorption energy increases as the overlap between adsorbate and surface increases.

The aim of this work is to evaluate, using a periodic DFT approach, the electronic changes produced by the sublayer doping of the MgO(100) and BaO(100) surfaces with a V, Ni, or Fe atom. The different atomic radii and electronegativities of the transition metal atoms give more insight about the structure and electronic changes produced by the doping in the AEMO structure. Electron density differences (EDD) are used to identify the electron density movement due to the doping.

2. Computational Details

Geometry optimizations were performed using the Vienna ab initio simulation program (VASP) [16, 17]. Kohn-Sham equations were solved with the generalized gradient approximation (GGA) proposed by Perdew and Wang [18]. The projector-augmented-wave (PAW) method of Blöchl [19] in the formulation of Kresse and Joubert [20] was applied to describe electron-ion interactions. Standard PAW potentials were used for Mg, Ba, Fe, V, Ni, and O with a valence electron distribution of $2s^2$, $5s^2 5p^6 6s^2$, $3d^7 4s^1$, $3d^4 4s^1$, $3d^9 4s^1$, and $2s^2 2p^4$, respectively. Brillouin-zone sampling was performed on Monkhorst-Pack special points [21] using a Methfessel-Paxton integration scheme. The plane-wave cutoff was set to 300 eV throughout all calculations except for the optimization of bulk unit cell parameters where at 400 eV plane-wave cutoff was used. This cutoff has shown to be high enough to reach sufficient convergence in this kind of systems [15].

The cubic MgO and BaO bulks were optimized starting from the experimental structure [22] with a k-point sampling of $4 \times 4 \times 4$ Monkhorst-Pack k-point mesh. The geometric parameters obtained were 4.236 and 5.604 Å for the MgO and BaO, respectively. The values obtained herein are in good agreement with the experimental parameters (4.211 and 5.523 Å for MgO and BaO, resp.) and with previous values obtained with a similar approach [1]. It is well known that a four-layer slab with a vacuum of the same thickness is enough to reach a surface energy convergence for these oxides [1]. In this work, the MgO(100) and BaO(100) surfaces were modelled with 2×2 five-layer slab (see Figure 1) where the two bottom layers were fixed to the optimized bulk structure and a vacuum separation of 13 Å thick was set between two periodically repeated slabs. The sublayer doped was carried out substituting one Mg or Ba atom of the second layer by one doping atom. We tested the effect of different spin multiplicity on the stability of the doped surface studies. All doped surfaces (both MgO(100) and BaO(100) surfaces) showed ferromagnetic arrangements of spin and we obtained a quadruplet, quintuplet, and triplet states for the V, Fe, and Ni doped surfaces, respectively.

The electronic structure was analyzed from the DOS plots and the electron charge distribution was examined by the Bader method [23, 24]. The EDD was plotted through

$$\Delta\rho = \rho_{(\text{surf+metal})} - \rho_{(\text{surf})} - \rho_{(\text{metal})}, \quad (1)$$

where $\rho_{(\text{surf+metal})}$ is the electron density of the adsorption surface plus the metal atom and $\rho_{(\text{surf})}$ and $\rho_{(\text{metal})}$ are the electron densities of the surface at the optimized adsorption positions and the metal atom, respectively. $\Delta\rho$ provides information on the electron redistribution upon the adsorption process. Thus, positive values correspond to density gain and negative values to density loss.

3. Results and Discussion

Table 1 displays the distances among the doping metals and the six nearest O atoms (one superficial (O_S), one in the bottom (O_B), and four equatorial (O_E)) for the MgO(100) and

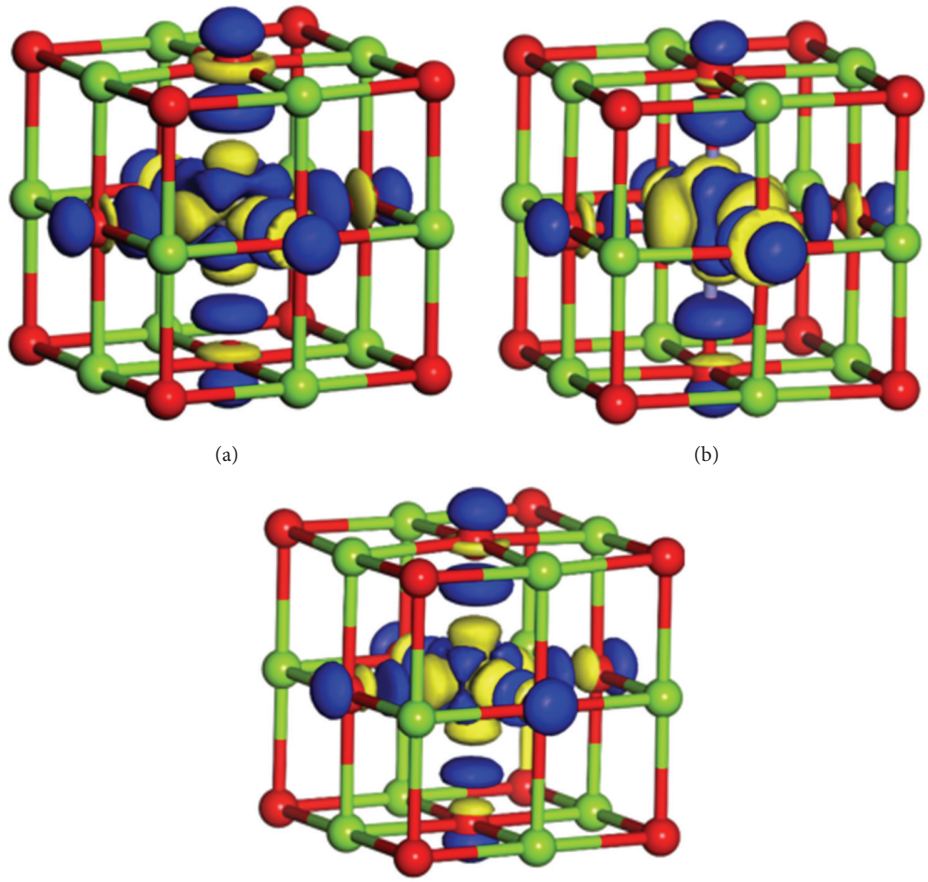

Figure 2: EDD for the V (a), Fe (b), and Ni (c) doped MgO(100) surfaces. The blue region corresponds to a density gain and the yellow region to a density loss. Oxygen atoms in red balls and metal atoms in green balls. For a better overview, only a $1 \times 1 \times 1$ cell was used.

Table 1: Equilibrium distances (Å) between the doping atom (Mg or Ba atom in the case of undoped surface) and the nearest O atoms. O_S corresponds to the superficial oxygen atom, O_E corresponds to the equatorial oxygen atoms, and O_B corresponds to the bottom oxygen atom.

	Oxygen atom	Mg or Ba	V	Fe	Ni
MgO	O_S	2.147	2.166	2.230	2.166
	O_E	2.118	2.140	2.143	2.131
	O_B	2.124	2.152	2.196	2.153
BaO	O_S	2.623	1.908	1.830	1.873
	O_E	2.803	2.257	2.774	2.789
	O_B	2.855	3.371	3.287	3.303

BaO(100) surfaces. For the MgO(100) surface, there is a little increase in all metal-O distances even in the case of the Ni atom in which covalent radius is smaller than the Mg atom (1.24 Å for the Ni atom and 1.41 Å for the Mg atom [25]). This is in good concordance with the experimental findings in Li doped MgO(100) surfaces; the Li-O distance increases [26–28] in comparison with the bulk Mg-O distance although the Li covalent radius (1.28 Å) is smaller than that of the Mg atom. It is evident that not only does the atom size play an important role in the structural changes observed in doped MgO(100) surfaces, but also bulk forces and electronic effects must affect the interaction between the doping atom and the O atoms. Nolan and Watson [29], using a similar approach to the one used in this work but with the PBE functional, found that the PBE functional produces a wrong description of the geometry and electronic structure of the doped MgO(100) surface. The results obtained in this work and those obtained with the same GGA functional [30, 31] seem to indicate that the PW91 functional performs much better than its homologous PBE functional for the study of structural properties of the doped MgO(100) surface. Due the largest cell vectors in the BaO(100) surface, the volume occupied by the Ba atom is big enough to avoid the optimal interaction among the doping atoms and the six O atoms. The doping atoms are nearest to the O_S atom (interaction distances below the 2 Å) and to the four O_E atoms in the case of the V atom. For Fe and Ni atoms, largest interaction distances are observed with respect to the O_E atoms suggesting that interaction is very weak. For the three doping atoms, distance with respect to the O_B atom

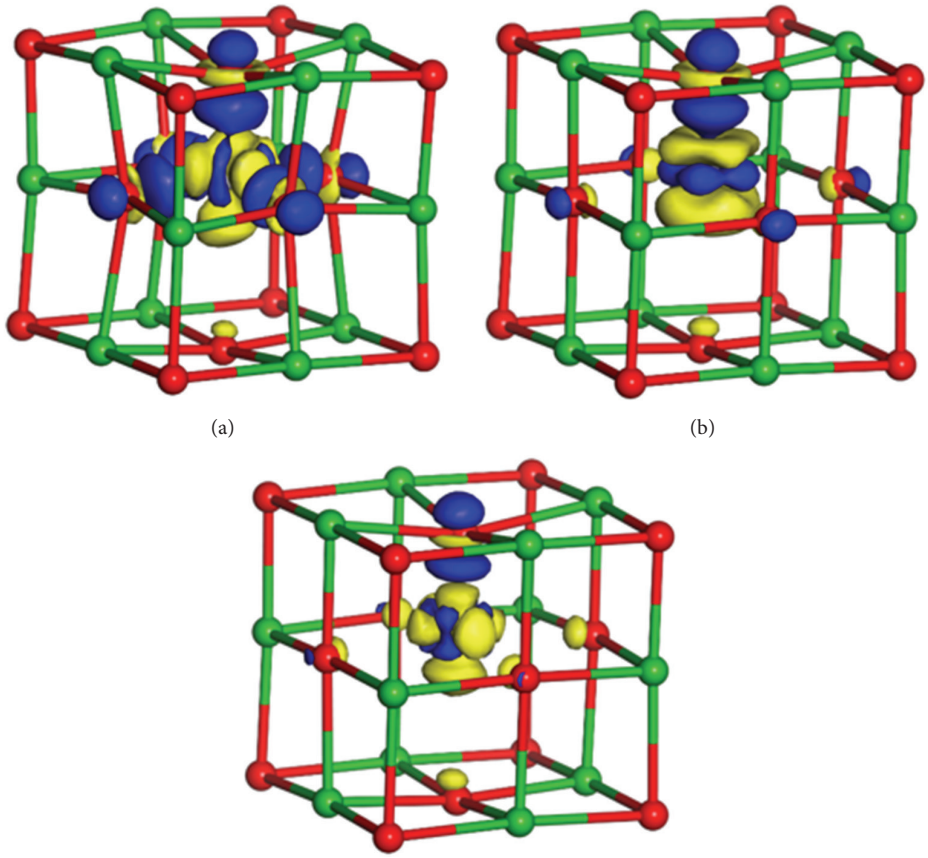

Figure 3: EDD for the V (a), Fe (b), and Ni (c) doped BaO(100) surfaces. The blue region corresponds to a density gain and the yellow region to a density loss. Oxygen atoms in red balls and metal atoms in green balls. For a better overview, only a $1 \times 1 \times 1$ cell was used.

is above 3.2 Å which indicates that there is no interaction between them.

The Bader analysis shows that the doping atoms transfer charge to the surface (see Table 2). In general, the charge transferred depends of the atom electronegative; that is, the more electronegative the atom, the less the charge transferred to the surface. V atom transfers approximately 1.5 e^- for both MgO(100) and BaO(100) surfaces; however, Fe and Ni atoms give less charge in the case of BaO(100) surface than in MgO(100) surface. Analyzing the EDD plots of the doped surfaces (see Figures 2 and 3) it is possible to observe that, for the MgO(100) surface, the three doping atoms interact with the six O atoms. This is consistent with the fact that covalent radii of the doping atoms are closer to that of the Mg atom (differences less than 0.17 Å); hence, the doping atoms fit very well in the Mg site. However in the case of the BaO(100) surface, where doping atoms seem to interact with only five O atoms, there is no electronic density movement in the interaction region among doping metals and the O_B atom; furthermore, for Fe and Ni the electron density difference is insignificant in the region between the metal and the O_E atoms. EDD plots corroborate the assumption made with the structural analysis; in the BaO(100) surface, the Fe and Ni atoms interact only with one O atom diminishing the possibility of transferring charge to the surface. Since Fe and Ni atoms lost approximately one e^-, these systems could be similar to those observed in Li doped MgO(100) surfaces (Li^+O^-) which have been reported to be responsible the promotion of reactions in oxidation of methane [32].

Table 2: The Bader charge analysis (e^-).

Atom	MgO	BaO
V	1.43	1.53
Fe	1.34	1.12
Ni	1.12	0.82

Figure 4 displays the total DOS for the doped MgO(100) surfaces. In a previous work [15], we noted that the valence band of the BaO(100) surface goes to low energy regions as the surface increases the electron reservoir, that is, from the undefected to the F_S surface (which has two electrons trapped in the defect). Observing the changes that occurred in the band structure of the doped MgO(100) surfaces, it can be seen that the doping atom introduces similar changes in the valence band than in the case of O defective surfaces. These changes are due to the inclusion of high energy states

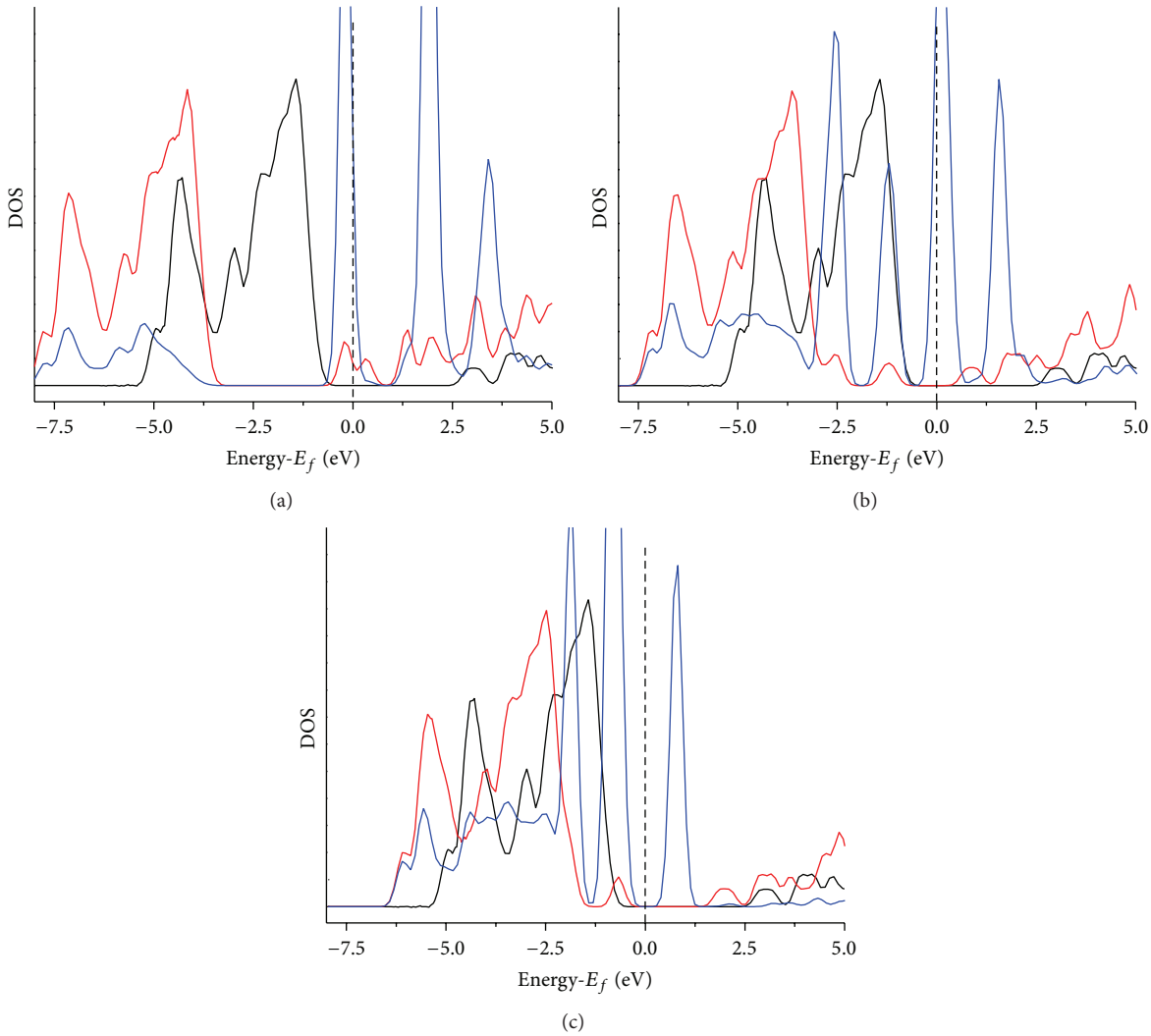

Figure 4: DOS of the V (a), Fe (b), and Ni (c) doped MgO(100) surfaces. In all cases, undoped, doped, and projected DOS of the doping atom are displayed with black, red, and blue lines, respectively. Only region near to the Fermi level is plotted for a better overview.

of the doping atom (see blue line in Figure 4) near the Fermi level. As the electron number of the doping atom increases, its electronic states near the Fermi level are more stable and closer among them (due to the crystal symmetry) resulting in less displacement of the valence band of the surface to low energy regions. Regardless of the doped surface, the nearest electronic states below the Fermi level belong to the doping atom. Displacement of the valence band to low energy regions is also observed in the case of the doped BaO(100) surfaces; however, in the case of Ni atom, the nearest electronic states below the Fermi level do not belong completely to the doping atom (see Figure 5). In addition to the s and p orbitals, the BaO(100) surface has $6d$ orbitals (from the Ba atom) closer to the Fermi level (see Figure 6). Then, electronic states from the Ni atom, some of which have energies near to the highest energy states of the Ba atom, pushes up to high energy regions part of the valence band of the surface. The nearest band below the Fermi level is now formed by electronic states of the doping atom and the surface. These results suggest that doping atoms not only introduce new electronic states near the Fermi level but also can move surface electronic states to the Fermi level increasing the ability of the doped surfaces to the adsorption of molecules with partially occupied states [15].

4. Conclusions

V, Fe, and Ni sublayer doped MgO(100) and BaO(100) surfaces were studied using a DFT periodic approach in the context of the PW91 functional. Our results indicate that PW91 functional performs well for the study of structural properties of the doped MgO(100) and BaO(100) surfaces. Doping atoms enclose very well in the sublayer of the MgO(100) surfaces; however, due to the higher covalent radius of the Ba atom, in the BaO(100) surface doping atoms accommodate near to the top layer displaying a strongest interaction with the O atom of the surface. The interaction

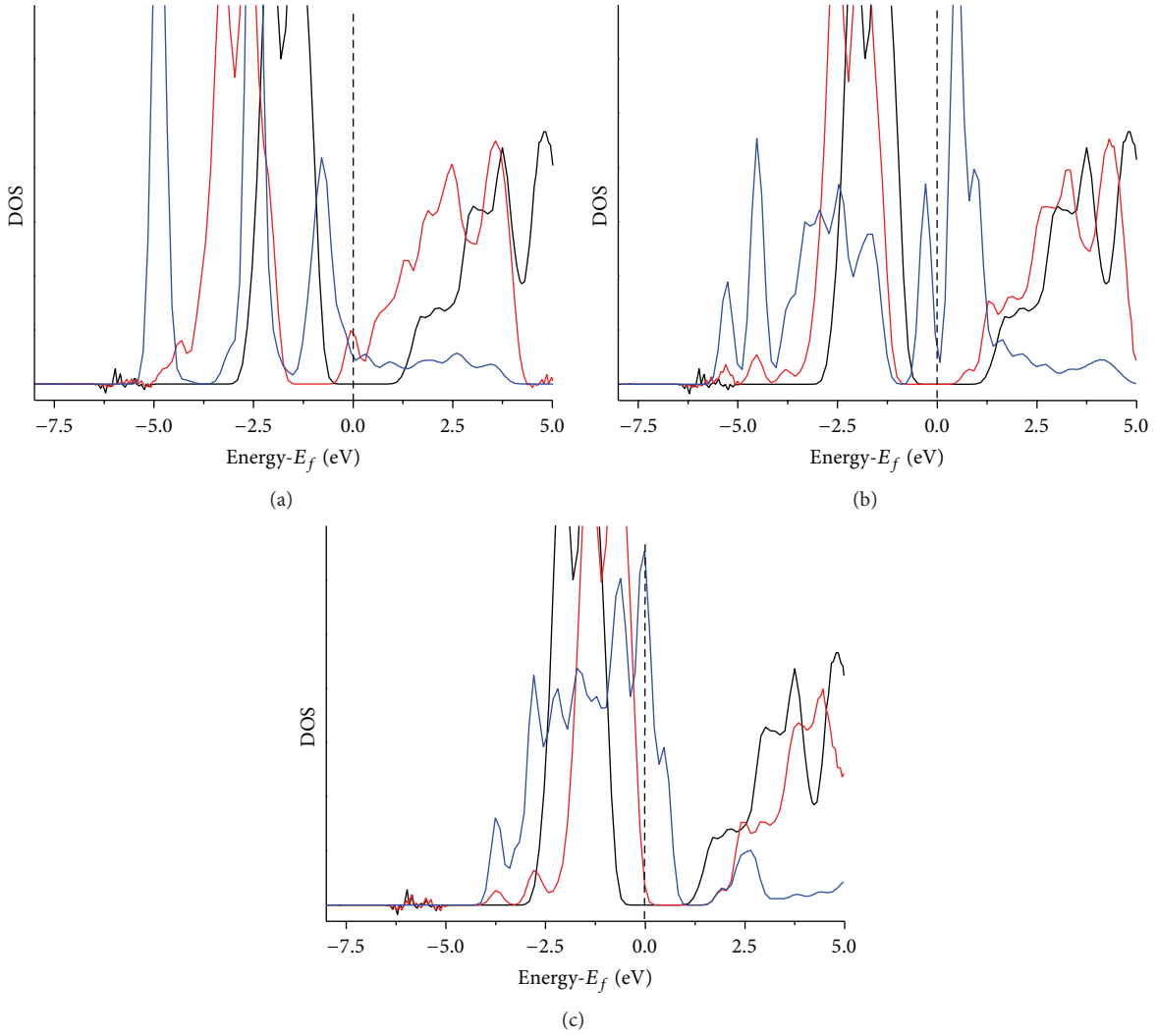

FIGURE 5: DOS of the V (a), Fe (b), and Ni (c) doped BaO(100) surfaces. In all cases, undoped, doped, and projected DOS of the doping atom are displayed with black, red, and blue lines, respectively. Only region near to the Fermi level is plotted for a better overview.

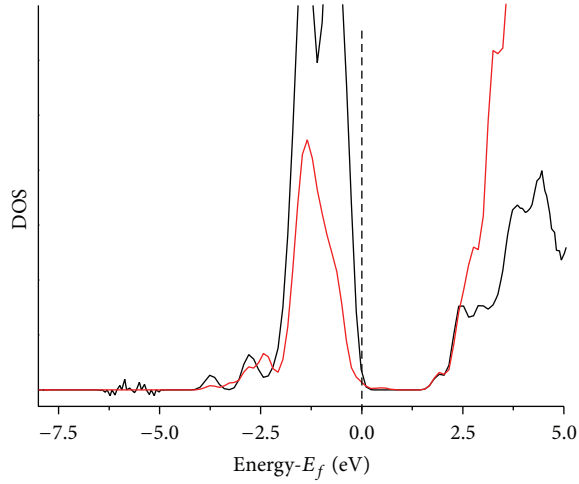

FIGURE 6: DOS of the Ni doped BaO(100) surface. Only region near to the Fermi level is plotted for a better overview. Total DOS in black line and the projected DOS of the *d* orbital of the surface Ba atom in red line.

of Fe and Ni in the BaO(100) surface could be similar to that observed in Li doped MgO(100) surfaces.

In general, doping atoms insert new electronic states near the Fermi level which move down the valence band of the surface to low energy regions. However, some orbitals of the Ni atom move up the higher electronic states of the BaO(100) surface. Then, the valence band near below the Fermi level is formed by electronic states of the surface and the doping atom which could improve the performance of the BaO(100) surface for trapping molecules with partially occupied states. Sizes of the doping atom, bulk forces, and electronic effects play an important role in the structural changes observed in doped MgO(100) and BaO(100) surfaces.

Conflict of Interests

The authors declare that there is no conflict of interests regarding the publication of this paper.

References

[1] W. F. Schneider, "Qualitative differences in the adsorption chemistry of acidic (CO_2, SO_x) and amphiphilic (NO_x) species on the alkaline earth oxides," *Journal of Physical Chemistry B*, vol. 108, no. 1, pp. 273–282, 2004.

[2] E. J. Karlsen, M. A. Nygren, and L. G. M. Pettersson, "Comparative study on structures and energetics of NO_x, SO_x, and CO_x adsorption on alkaline-earth-metal oxides," *The Journal of Physical Chemistry B*, vol. 107, no. 31, pp. 7795–7802, 2003.

[3] G. Pacchioni, J. M. Ricart, and F. Illas, "Ab initio cluster model calculations on the chemisorption of CO_2 and SO_2 probe molecules on MgO and CaO (100) surfaces. A theoretical measure of oxide basicity," *Journal of the American Chemical Society*, vol. 116, no. 22, pp. 10152–10158, 1994.

[4] H. Matsuhashi, M. Oikawa, and K. Arata, "Formation of superbase sites on alkaline earth metal oxides by doping of alkali metals," *Langmuir*, vol. 16, no. 21, pp. 8201–8205, 2000.

[5] A. M. Ferrari and G. Pacchioni, "Electronic structure of F and V centers on the MgO surface," *Journal of Physical Chemistry*, vol. 99, no. 46, pp. 17010–17018, 1995.

[6] T. Iizuka, Y. Endo, H. Hattori, and K. Tanabe, "Unusually strong basic sites as active sites for Cis–Trans interconversion of 2-butene on CaO," *Chemistry Letters*, vol. 5, no. 8, pp. 803–804, 1976.

[7] P. Raschman and A. Fedoročková, "Dissolution kinetics of periclase in dilute hydrochloric acid," *Chemical Engineering Science*, vol. 63, no. 3, pp. 576–586, 2008.

[8] H. Kurokawa, T. Kato, W. Ueda, Y. Morikawa, Y. Moro-oka, and T. Ikawa, "Solid base-catalyzed reaction of nitriles with methanol to form α,β-unsaturated nitriles I. Conversion and selectivity," *Journal of Catalysis*, vol. 126, no. 1, pp. 199–207, 1990.

[9] H. Kurokawa, T. Kato, T. Kuwabara et al., "Solid base-catalyzed reaction of nitriles with methanol to form α,β-unsaturated nitriles II. Surface base property and reaction mechanism," *Journal of Catalysis*, vol. 126, no. 1, pp. 208–218, 1990.

[10] W.-Z. Li, K.-Q. Sun, Z. Hu, and B.-Q. Xu, "Characteristics of low platinum Pt–BaO catalysts for NOx storage and reduction," *Catalysis Today*, vol. 153, no. 3-4, pp. 103–110, 2010.

[11] W. S. A. Halim, M. M. Assem, A. S. Shalabi, and K. A. Soliman, "CO adsorption on Ni, Pd, Cu and Ag deposited on MgO, CaO, SrO and BaO: density functional calculations," *Applied Surface Science*, vol. 255, no. 17, pp. 7547–7555, 2009.

[12] J. Baltrusaitis, C. Hatch, and R. Orlando, "Periodic DFT study of acidic trace atmospheric gas molecule adsorption on Ca- and Fe-doped MgO(001) surface basic sites," *Journal of Physical Chemistry A*, vol. 116, no. 30, pp. 7950–7958, 2012.

[13] B. J. Wuensch and T. Vasilos, "Diffusion of transition metal ions in single-crystal MgO," *The Journal of Chemical Physics*, vol. 36, no. 11, pp. 2917–2922, 1962.

[14] E. B. Rigby and I. B. Cutler, "Interdiffusion studies of the system Fe_xO-MgO," *Journal American Ceramic Society*, vol. 48, pp. 95–99, 1965.

[15] R. Añez, A. Sierraalta, A. Bastardo, D. Coll, and B. Garcia, "Density functional study of NO adsorption on undefected and oxygen defective Au–BaO(1 0 0) surfaces," *Applied Surface Science*, vol. 307, pp. 165–171, 2014.

[16] G. Kresse and J. Hafner, "Ab initio molecular dynamics for liquid metals," *Physical Review B*, vol. 47, no. 1, pp. 558–561, 1993.

[17] G. Kresse and J. Furthmüller, "Efficient iterative schemes for ab initio total-energy calculations using a plane-wave basis set," *Physical Review B*, vol. 54, no. 16, pp. 11169–11186, 1996.

[18] J. P. Perdew and Y. Wang, "Accurate and simple analytic representation of the electron-gas correlation energy," *Physical Review B*, vol. 45, no. 23, pp. 13244–13249, 1992.

[19] P. E. Blöchl, "Projector augmented-wave method," *Physical Review B*, vol. 50, no. 24, pp. 17953–17979, 1994.

[20] G. Kresse and D. Joubert, "From ultrasoft pseudopotentials to the projector augmented-wave method," *Physical Review B—Condensed Matter and Materials Physics*, vol. 59, no. 3, pp. 1758–1775, 1999.

[21] H. J. Monkhorst and J. D. Pack, "Special points for Brillouin-zone integrations," *Physical Review B*, vol. 13, article 5188, 1976.

[22] V. E. Henrich and P. A. Cox, *The Surface Science of Metal Oxides*, Cambridge University Press, Cambridge, UK, 1994.

[23] R. F. W. Bader, "A quantum theory of molecular structure and its applications," *Chemical Reviews*, vol. 91, no. 5, pp. 893–928, 1991.

[24] R. F. W. Bader, *Atoms in Molecules: A Quantum Theory*, Clarendon Press, Oxford, UK, 1990.

[25] B. Cordero, V. Gómez, A. E. Platero-Prats et al., "Covalent radii revisited," *Dalton Transactions*, no. 21, pp. 2832–2838, 2008.

[26] M. M. Abraham, W. P. Unruh, and Y. Chen, "Electron-nuclear-double-resonance investigations of $[Li]^0$ and $[Na]^0$ centers in MgO, CaO, and SrO," *Physical Review B*, vol. 10, no. 8, pp. 3540–3545, 1974.

[27] M. M. Abraham, Y. Chen, L. A. Boatner, and R. W. Reynolds, "Stable $[Li]^0$ defects in MgO single crystals," *Physical Review Letters*, vol. 37, no. 13, pp. 849–852, 1976.

[28] Y. Chen, H. T. Tohver, J. Narayan, and M. M. Abraham, "High-temperature and ionization-induced effects in lithium-doped MgO single crystals," *Physical Review B*, vol. 16, no. 12, pp. 5535–5542, 1977.

[29] M. Nolan and G. W. Watson, "The electronic structure of alkali doped alkaline earth metal oxides: Li doping of MgO studied with DFT-GGA and GGA + U," *Surface Science*, vol. 586, no. 1–3, pp. 25–37, 2005.

[30] Z. X. Yang, G. Liu, and R. Q. Wu, "Effects of Li impurities on MgO(100)," *Physical Review B*, vol. 65, no. 23, Article ID 235432, 2002.

[31] L. K. Dash and M. J. Gillan, "Assessment of competing mechanisms of the abstraction of hydrogen from CH_4 on Li/MgO(0 0 1)," *Surface Science*, vol. 549, no. 3, pp. 217–226, 2004.

[32] J. H. Lunsford, "The catalytic conversion of methane to higher hydrocarbons," *Catalysis Today*, vol. 6, no. 3, pp. 235–259, 1990.